the plant journal

SEB Society for Experimental Biology

The Plant Journal (2014) **78,** 706–714 doi: 10.1111/tpj.12499

TECHNICAL ADVANCE

ISWI proteins participate in the genome-wide nucleosome distribution in Arabidopsis

Guang Li[†,‡], Shujing Liu[†], Jiawei Wang, Jianfeng He, Hai Huang, Yijing Zhang* and Lin Xu*

National Laboratory of Plant Molecular Genetics, Institute of Plant Physiology and Ecology, Shanghai Institutes for Biological Sciences, Chinese Academy of Sciences, 300 Fenglin Road, Shanghai 200032, China

Received 11 November 2013; revised 28 January 2014; accepted 24 February 2014; published online 8 March 2014.
*For correspondence (e-mails zhangyijing@sibs.ac.cn or xulin01@sibs.ac.cn).
[†]Authors contributed equally to this work.
[‡]Present address: Stanford Cardiovascular Institute, Stanford University School of Medicine, Stanford, CA 94305, USA.

SUMMARY

Chromatin is a highly organized structure with repetitive nucleosome subunits. Nucleosome distribution patterns, which contain information on epigenetic controls, are dynamically affected by ATP-dependent chromatin remodeling factors (remodelers). However, whether plants have specific nucleosome distribution patterns and how plant remodelers contribute to the pattern formation are not clear. In this study we used the micrococcal nuclease digestion followed by deep sequencing (MNase-seq) assay to show the genome-wide nucleosome pattern in *Arabidopsis thaliana.* We demonstrated that the nucleosome distribution patterns of Arabidopsis are associated with the gene expression level, and have several specific characteristics that are different from those of animals and yeast. In addition, we found that remodelers in the *A. thaliana* imitation switch (AtISWI) subfamily are important for the formation of the nucleosome distribution pattern. Double mutations in the AtISWI genes, *CHROMATIN REMODELING 11* (*CHR11*) and *CHR17*, resulted in the loss of the evenly spaced nucleosome pattern in gene bodies, but did not affect nucleosome density, supporting a previous idea that the primary role of ISWI is to slide nucleosomes in gene bodies for pattern formation.

Keywords: Nucleosome distribution, ISWI, ATP-dependent chromatin remodeling, MNase-seq, *Arabidopsis thaliana*, technical advance.

INTRODUCTION

Chromatin, which is composed of repetitive units called nucleosomes, is the template that harbors epigenetic information on how to spatially and temporally transcribe genes in addition to the genetic information, and thus changes in chromatin organization alter gene expression (Russo *et al.*, 1996). In eukaryotes, nucleosomes are not distributed randomly along the chromatin, but rather in a regular and controlled pattern (Bai and Morozov, 2010; Sadeh and Allis, 2011; Struhl and Segal, 2013). Studies on genome-wide and locus-specific nucleosome distribution patterns in yeast and animals revealed that such patterns are correlated with transcription levels, providing important evidence that a specific nucleosome distribution pattern contains epigenetic information that directs gene expression (Shivaswamy *et al.*, 2008; Weiner *et al.*, 2010; Yadon *et al.*, 2010; Sala *et al.*, 2011; Fu *et al.*, 2012; Gaffney *et al.*, 2012; Li *et al.*, 2012b; Chen *et al.*, 2013).

ATP-dependent chromatin remodeling factors (remodelers), which belong to the Snf2 ATPase family, play critical roles in the dynamic packaging or unpackaging of chromatin, using energy from ATP hydrolysis (for review see Clapier and Cairns (2009)). Remodelers change the contacts between histones and DNA in the nucleosome, allowing them to arrange the distribution pattern of nucleosome spacing along the chromatin. Thus, it is thought that remodelers play key roles in the activation or repression of gene expression, and are essential for physiology and/or development in yeast, animals and plants. The Arabidopsis genome contains 41 genes that encode such ATPase remodelers, some of which are known to act as important epigenetic regulators (Knizewski *et al.*, 2008). The imitation switch (ISWI)-type chromatin remodeling factors belong to a subfamily of these remodelers, and the *Arabidopsis thaliana* ISWI (AtISWI) proteins CHROMATIN REMODELING 11

(CHR11) and CHR17 are involved in multiple developmental processes, including female gametogenesis (Huanca-Mamani *et al.*, 2005), flowering time control (Li *et al.*, 2012a) and flower development (Smaczniak *et al.*, 2012). In addition, AtISWI has been shown to form complexes with the AtDDT-domain proteins for regulating specific target genes (Aravind and Iyer, 2012; Li *et al.*, 2012a; Smaczniak *et al.*, 2012; Dong *et al.*, 2013).

However, our knowledge about genome-wide nucleosome distribution patterns and the relationship between gene transcription levels and the nucleosome distribution patterns in plants is limited. Importantly, the biochemical basis of how plant remodelers are involved in such pattern formation is unknown. In this study, we used the micrococcal nuclease digestion followed by deep sequencing (MNase-seq) assay to address the genome-wide organization of the nucleosome distribution in Arabidopsis and the *in vivo* role of AtISWI in the formation of nucleosome distribution patterns. Finally, we propose models to explain the differences in nucleosome distribution patterns among plants, yeast and animals, and the common and distinct functions of ISWI in Arabidopsis and *Drosophila.*

RESULTS

Nucleosome distribution patterns of different gene types in wild-type plants

We performed an micrococcal nuclease digestion followed by deep sequencing (MNase-seq) assay to analyse the nucleosome distribution in Arabidopsis (Figure 1). For quality control, we examined the MNase-seq read distribution around replication origins (Costas *et al.*, 2011) and DNase I hypersensitive sites (DHS) (Zhang *et al.*, 2012), the latter of which represent the nucleosome-free region (Figure S1). The quality control showed that the raw reads were dramatically low in the DHS and accumulated around replication origins, which is consistent with the previous knowledge of nucleosome distribution in Arabidopsis (Costas *et al.*, 2011; Zhang *et al.*, 2012), indicating that our MNase-seq raw data are suitable for nucleosome distribution pattern analysis. To identify the position of nucleosomes, the raw reads were processed by the TEMPLATE FILTER software, which used seven empirical nucleosome positioning models as templates to detect potential nucleosome positions and remove other uncorrelated reads as background (Weiner *et al.*, 2010) (Figure S2; for details, see Experimental Procedures).

To find patterns of nucleosome distribution in different types of genes in wild-type Columbia-0 (Col-0) seedlings, we analysed separately four groups of sequences: protein-coding genes, pseudogenes, transposable elements (TEs) and TE genes. The chosen analysis region was from −1000 bp upstream (1-kb promoter) to +1000 bp downstream (1-kb gene body) of the transcription start site (TSS) for protein-coding genes or the 5′ boundary for pseudogenes, TEs and TE genes, because this region covers most of the transcription information in the genome and has been commonly chosen for analysis of nucleosome distribution (Shivaswamy *et al.*, 2008; Weiner *et al.*, 2010; Sala *et al.*, 2011).

Whole-genome statistical analysis of 27 416 protein-coding genes displayed a typical nucleosome distribution pattern surrounding the TSS. Firstly, a relatively low nucleosome density was found in the 1-kb promoter regions and a relatively high nucleosome density was found in the 1-kb gene bodies (Figure 2a). This pattern is consistent with the previous results of nucleosome analysis and prediction (Chodavarapu *et al.*, 2010; Fincher *et al.*, 2013). Secondly, an evenly spaced nucleosome distribution with a period of approximately 160 bp was found in the 1-kb gene bodies (Figure 2a).

There were 924 pseudogenes and 3903 TE genes that also displayed a relatively low nucleosome density in the 1-kb promoter region and a high density in the 1-kb gene bodies, but the evenly spaced nucleosome distribution as shown in the 1-kb gene bodies of coding genes was not observed (Figure 2b,c). These results suggest that the evenly spaced nucleosome distribution in the 1-kb gene bodies may be associated with genes that have the potential ability to transcribe.

Although pseudogenes and TE genes retain a relatively low nucleosome density in the 1-kb promoter regions compared with their own gene bodies, the nucleosome density of the 1-kb promoter regions is much higher than that of protein-coding genes, especially within the regions close to the 5′ boundary (Figure 2e). In addition, we performed statistical analysis of the nucleosome read coverage on the whole gene bodies from the TSS or the 5′ boundary to the transcription end site (TES) or the 3′ boundary and the 1-kb promoters. The nucleosome density in the 1-kb promoters of TE genes and pseudogenes is significantly higher than that of protein-coding genes, while that in the whole gene bodies of TE genes is slightly higher than that of protein-coding genes (Figure 2f,g). Taken together, these data suggest that the 1-kb promoter regions of protein-coding genes are much more open than pseudogenes and TE genes, and the high nucleosome read density in promoters of pseudogenes and TE genes may be related to their expression silencing.

Unlike protein-coding genes, TE genes and pseudogenes, TEs did not show an obvious regular distribution pattern of nucleosomes (Figure 2d,e). It is notable that the nucleosome occupancy of protein-coding genes in the 500-bp region upstream of the TSS is lower than that in TEs (Figure 2e).

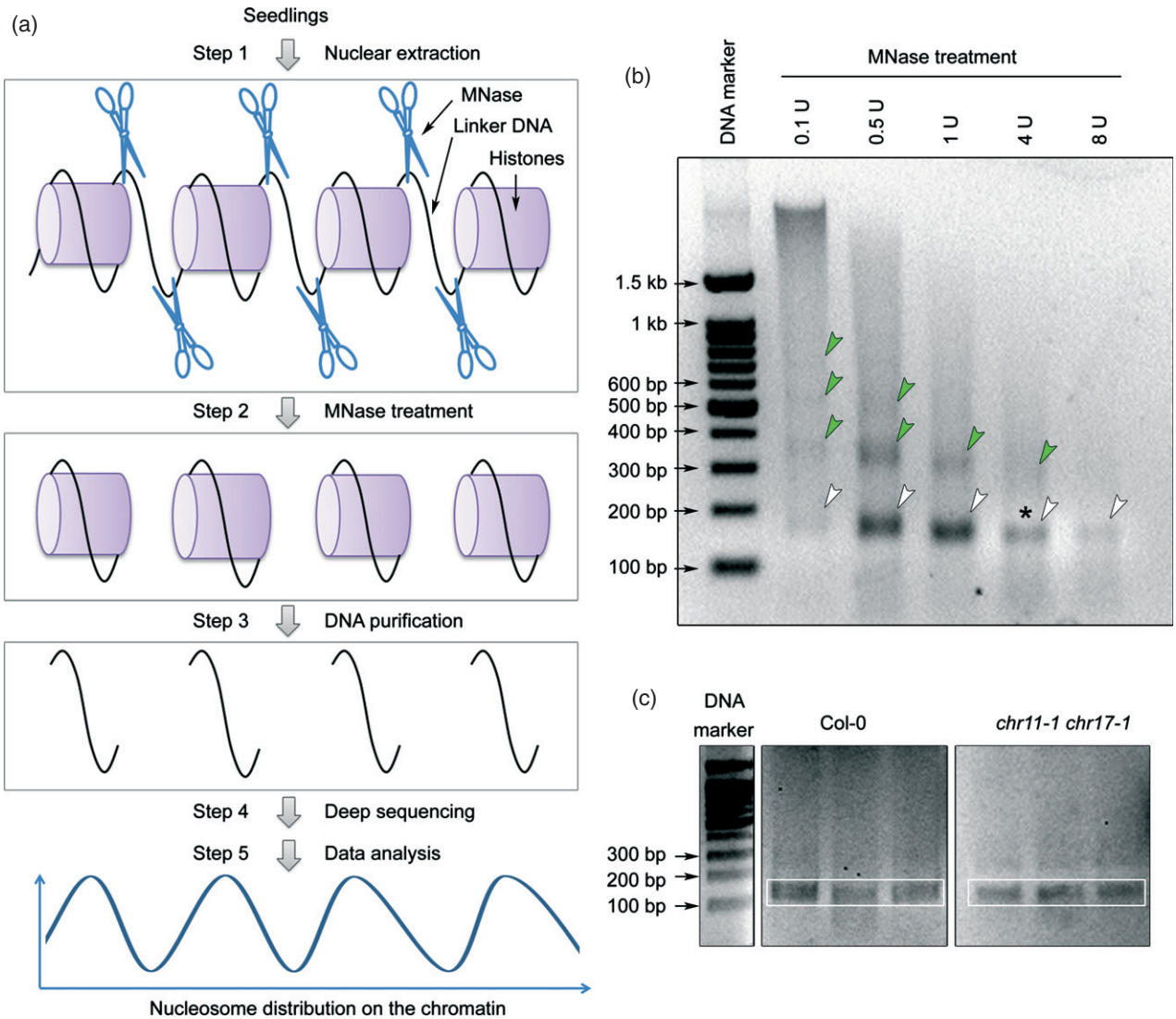

Figure 1. Micrococcal nuclease digestion followed by deep sequencing (MNase-seq) analysis of nucleosome features.
(a) An illustration of the MNase-seq experiment. Because the linear DNA was digested by MNase, DNA wrapped on histones of mononucleosomes was less attacked by MNase, and represents the nucleosome positions in the genome.
(b) Different titration levels of MNase in the reaction of extracted nuclei. After treatment of extracted nuclei with MNase, chromatin was digested into oligo-, di-, and mononucleosomes based on different MNase levels in the reaction. MNase levels from 0.8 U to 8 U were tested to optimize the reaction. An appropriate level of 4 U of MNase was chosen, because at this concentration the mononucleosomes (within 100–200 bp) are most suitable for deep sequencing analysis according to a previous report (Weiner *et al.*, 2010). The bands on the gel show di- and oligonucleosomes (green arrowheads), and mononucleosomes (white arrowheads). The asterisk indicates the appropriately digested mononucleosomes.
(c) Nuclei from wild-type Col-0 and *chr11-1 chr17-1* were treated with MNase and the boxed DNA bands were purified for deep sequencing.

Nucleosome distribution patterns are associated with gene expression levels

We further classified the protein-coding genes into four categories according to their expression levels based on our previously published Col-0 microarray data (Li *et al.*, 2012a): 5626 highly expressed genes, 4780 relatively highly expressed genes, 5269 relatively lowly expressed genes, and 5627 lowly expressed genes (Figure S3). Our data showed that the pattern, in which the low nucleosome occupancy is in the 1-kb promoter regions and the high occupancy is in the 1-kb gene bodies, was present in all categories of genes (Figure 3a–e), which suggested that this pattern is a basic one of all protein-coding genes regardless of expression levels. However, the pattern of evenly spaced nucleosome distribution in the 1-kb gene bodies closely correlated with transcription levels. The higher the transcription level, the more prominent the evenly spaced nucleosome pattern was (Figure 3a–e). We found that the nucleosome distribution pattern of the lowly expressed genes (Figure 3d) was similar to that of the

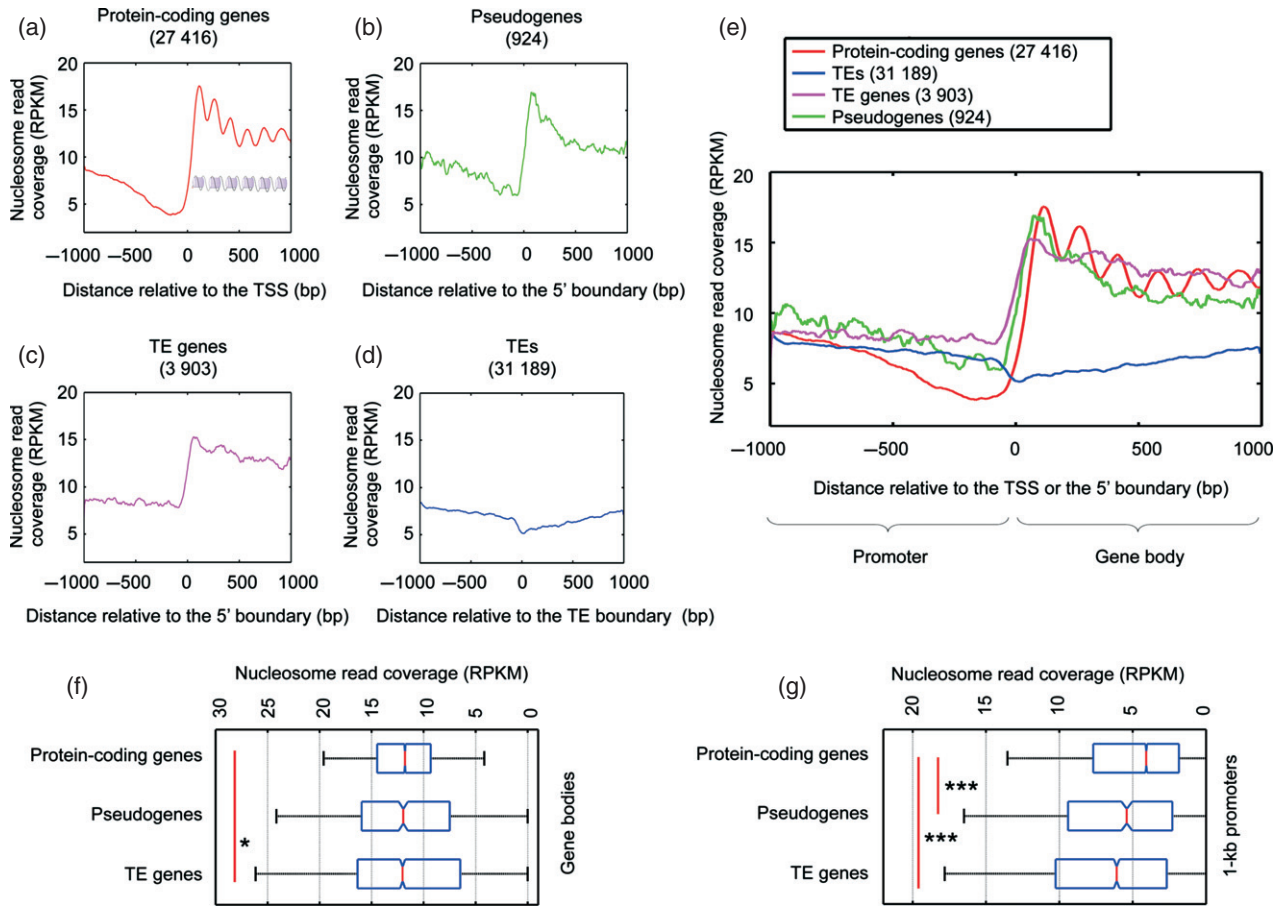

Figure 2. Genome-wide nucleosome distribution patterns of different types of genes and transposable elements (TEs) in wild-type Col-0.
(a–d) Nucleosome distribution patterns of protein-coding genes (a), pseudogenes (b), TE genes (c) and TEs (d) surrounding the transcription start site (TSS).
(e) Merged image of (a–d).
(f, g) Nucleosome read coverage on gene bodies (f) and on 1-kb promoters (g) of different types of genes. *$P < 0.05$; ***$P < 0.001$ in a two-sample *t*-test.

pseudogenes and TE genes (Figure 2b,c), further supporting the hypothesis that genes with evenly spaced nucleosomes within the 1-kb gene bodies are closely correlated with their high transcription levels.

Next, we analysed statistically the nucleosome read coverage on the whole gene bodies (from the TSS to TES), 1-kb promoters and the upstream and downstream 200-bp regions adjacent to the TSS (TSS region) of genes with different expression levels. The nucleosome density negatively associated with gene expression levels in the whole gene bodies, but not in the 1-kb promoters (Figure 3f,g). Within the TSS regions, the nucleosome density also negatively correlated with the gene expression level (Figure 3h). These observations are consistent with the previous results (van Dijk *et al.*, 2010; Stroud *et al.*, 2012) that the open state of gene bodies and the TSS regions correlates with gene transcription.

A more detailed analysis revealed that the position of the first nucleosome 3′ adjacent to the TSS also correlated closely with gene expression levels. The higher the gene expression levels, the further away the first nucleosome is from the TSS (Figure 3i). The Kolmogorov–Smirnov test showed that the nucleosome distribution between adjacent groups is significantly different (Figure 3j). These results suggest that high transcription levels of genes require the first nucleosome to be far away from the TSS; or alternatively, transcription may push the +1 nucleosome further into the transcribed region, thus retaining a relatively open chromatin state for transcription machineries.

AtISWI is required for nucleosome spacing in gene bodies

To understand the role of AtISWI remodelers in nucleosome patterning, we compared the MNase-seq data of the AtISWI double mutant *chr11-1 chr17-1* with that of the wild-type. The basic pattern of low nucleosome density in the promoter regions and high occupancy in the gene bodies in wild-type was similar to that in *chr11-1 chr17-1* for the 27 416 protein-coding genes analysed (Figure 4a), suggesting that AtISWI does not contribute to this basic pattern. Interestingly, although the first nucleosome

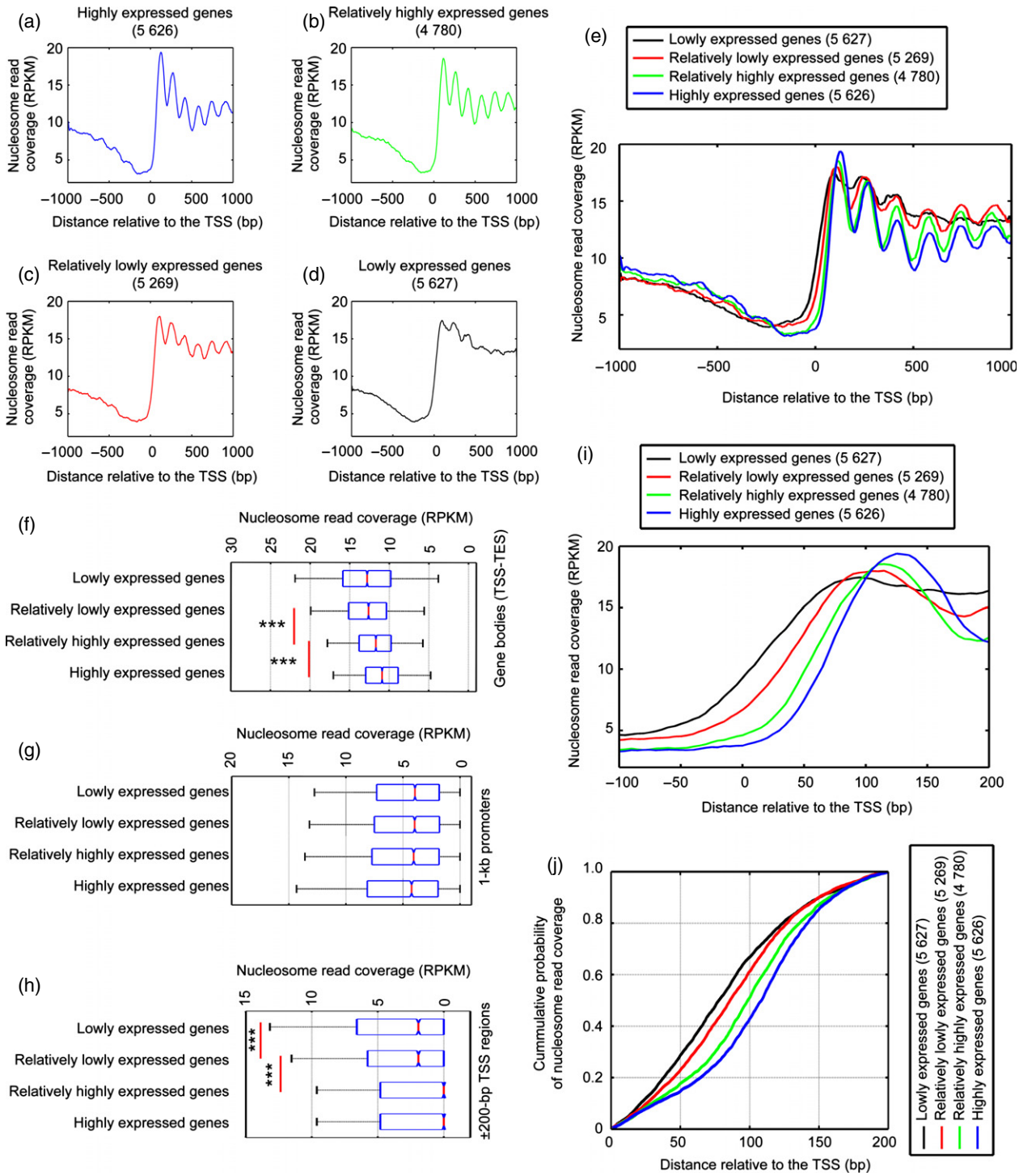

Figure 3. Genome-wide nucleosome distribution patterns of genes with different expression levels in wild-type Col-0.
(a–d) Nucleosome distribution patterns of highly (a), relatively highly (b), relatively lowly (c) and lowly (d) expressed genes surrounding the transcription start site (TSS).
(e) Merged image of (a–d).
(f–h) Nucleosome read coverage on gene bodies from the TSS to the transcription end site (TES) (f), on 1-kb promoters (g), and on the TSS regions (h) of genes with different expression levels. ***$P < 0.001$ in two-sample *t*-test.
(i) Zoom-in view of (e) around the TSS.
(j) Cumulative distribution of the distance between the TSS and the first nucleosome in gene bodies for each group. The distance was weighted by the number of reads associated with +1 nucleosome, which provides the confidence for the existence of a given nucleosome. The Kolmogorov–Smirnov test was used to test the equality of the distribution between each adjacent group, and the difference is significant for each test ($P < 0.001$).

position was not altered in *chr11-1 chr17-1*, the evenly spaced nucleosome distribution pattern in gene bodies was obviously changed (Figure 4a). The position and density of the first nucleosome downstream to the TSS in *chr11-1 chr17-1* were similar to those in wild-type. However, the position of the second and third nucleosomes was less prominent in *chr11-1 chr17-1* compared with that in wild-type, and regularly arranged nucleosomes after the third one were barely present in *chr11-1 chr17-1.* These results indicated that AtISWI is involved in the patterning of the evenly spaced nucleosomes in protein-coding gene bodies. No obvious difference in nucleosome patterns in pseudogenes, TE genes and TEs was found between wild-type and the *chr11-1 chr17-1* mutant (Figure S4).

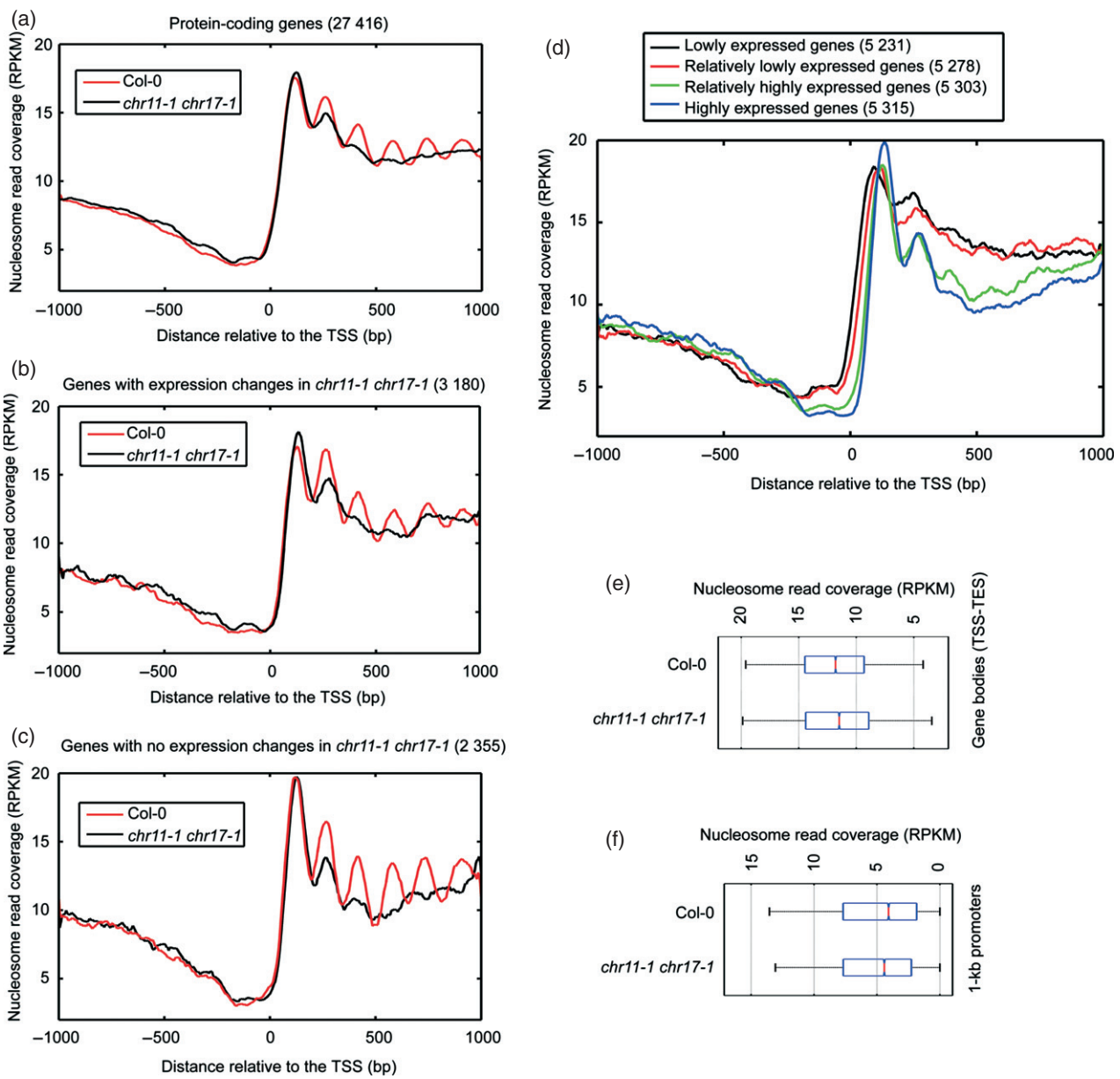

Figure 4. AtISWI is required for regular spacing of nucleosomes in gene bodies.
(a) Nucleosome distribution patterns of protein-coding genes in wild-type Col-0 (black line) and *chr11-1 chr17-1* (red line).
(b, c) Nucleosome distribution patterns of the expression-altered (b) or unaffected (c) protein-coding genes in wild-type Col-0 (black line) and *chr11-1 chr17-1* (red line). In this study, genes with altered expression levels were defined as $\geq \pm$ 1.5-fold (*chr11-1 chr17-1* versus Col-0), $P < 0.01$. Genes with unaffected expression levels were defined as $\leq \pm$ 1.1-fold, $P < 0.01$.
(d) Nucleosome distribution patterns of highly, relatively highly, relatively lowly and lowly expressed genes surrounding the TSS in *chr11-1 chr17-1.*
(e, f) Nucleosome read coverage on gene bodies from the TSS to the TES (e) and on 1-kb promoters (f) of wild-type Col-0 and *chr11-1 chr17-1.*

We next tested whether AtISWI directly affects the nucleosome distribution or only the gene expression profiles, which in turn affect nucleosome distribution. Based on gene expression levels using our previous microarray data (Li *et al.*, 2012a), 3180 genes showed altered expression levels in *chr11-1 chr17-1* compared with those in wild-type Col-0, whereas 2355 were unaffected (Figures 4b,c and S5). Our results revealed that the nucleosome distribution patterns of the two groups of genes were all affected by loss of AtISWI functions (Figures 4b,c and S5), which suggested that the nucleosome arrangement function of AtISWI is independent of and prior to gene transcription. In addition, the first nucleosome is more evident in the unaffected genes in the double mutant (Figure 4c).

Furthermore, we classified the protein-coding genes into four categories according to their expression levels determined by our previously published *chr11-1 chr17-1* microarray data (Li *et al.*, 2012a). There are 5231 lowly expressed genes, 5278 relatively lowly expressed genes, 5303 relatively highly expressed genes and 5315 highly expressed genes in the *chr11-1 chr17-1* background (Figure S3). Our data showed that the higher the transcription level, the more evident the position of the first and second evenly spaced nucleosomes is in gene bodies (Figure 4d). These results suggest that a correlation between the evenly spaced nucleosome pattern in gene bodies and the gene transcription levels is still present in the *chr11-1 chr17-1* mutant, whereas the even distribution pattern is impaired in each of these gene groups.

Finally, we statistically analysed the nucleosome read coverage on gene bodies (from the TSS to TES) and the 1-kb promoter regions of protein-coding genes of wild-type and *chr11-1 chr17-1.* Our data showed that the number of nucleosome reads in both gene bodies and promoters was not statistically different between wild-type and *chr11-1 chr17-1* (Figure 4e,f), suggesting that AtISWI does not control the overall nucleosome density.

DISCUSSION

In this study, we identified the Arabidopsis nucleosome distribution patterns from the genome-wide scale, and also explored their relationship with gene types and the gene expression level. Our data showed that Arabidopsis has several unique nucleosome distribution patterns, which are not fully consistent with those from yeast and animals. In Arabidopsis, promoter regions usually have low nucleosome density with the lowest at the TSS, whereas in yeast the corresponding regions have relatively high nucleosome occupancy, with several evenly spaced nucleosomes in the promoters (Shivaswamy *et al.*, 2008). A relatively high nucleosome density was also observed in the 500-bp promoter region immediately upstream of the TSS in *Drosophila* (Sala *et al.*, 2011). Another difference between yeast and Arabidopsis is that yeast genes that are expressed at low levels usually have a more evenly spaced nucleosome pattern in gene bodies compared with the highly expressed genes (Shivaswamy *et al.*, 2008). This pattern is opposite to the pattern of Arabidopsis. We propose that the difference between Arabidopsis and yeast may stem from diverse mechanisms that regulate gene expression. In addition, because the length of the DNA per nucleosome may be quite different between these organisms, this difference might also account for the difference of nucleosome patterns.

ATP-dependent chromatin remodeling factors were thought to assemble nucleosomes via two major ways: sliding and depositing or ejecting nucleosomes (Clapier and Cairns, 2009). In addition, regular spacing of nucleosomes is a common action of ISWI remodeler (Langst and Becker, 2001; Gkikopoulos *et al.*, 2011). Our study provides additional *in vivo* evidence that AtISWI acts in sliding nucleosomes in gene bodies. Because the nucleosome density is similar in wild-type and the *chr11-1 chr17-1* mutant, the primary role of AtISWI may not be involved in the deposition or ejection of nucleosomes. We showed the direct AtISWI effect on the generation of the evenly spaced nucleosome pattern in gene bodies (see a model in Figure S6). It is possible that sliding nucleosomes is a fundamental role that ISWI plays, which is conserved between animals and plants. It has been shown that the *Drosophila* ISWI generates an evenly spaced structure of the nucleosome in an *in vitro* biochemical assay (Narlikar, 2010), and *in vivo* data have shown that *Drosophila* ISWI slides the first two nucleosomes in gene bodies (Sala *et al.*, 2011). All these data, together with the fact that the ISWI proteins have very conserved structures among eukaryotes (Yadon and Tsukiyama, 2011), suggest that the function of ISWI is conserved at the biochemical level. However, some minor differences of the ISWI function were also present in Arabidopsis and *Drosophila.* For example, *Drosophila* ISWI functions not only surrounding the TSS but also at the TES (Sala *et al.*, 2011). Besides, the AtISWI mutant also showed increased nucleosome read density in the middle of DHS (Figure S1), which suggested the possible role of AtISWI in controlling the nucleosome positioning around these potential regulatory sites. Therefore, each species may have some minor differences of the ISWI function *in vivo.*

We could not exclude the possibility that AtISWI has a function in sliding nucleosomes in pseudogenes, TEs, TE genes and the promoter regions of protein-coding genes, although a regular nucleosome distribution pattern was not observed in these genomic regions in wild-type and in the loss-of-function AtISWI mutant. Because these regions do not show a regular nucleosome distribution pattern, we are currently unable to extract information about how AtISWI remodels nucleosomes in these regions. The yeast Isw2 protein has been shown to be involved in the regulation of nucleosome positioning in many gene regions

(Yadon *et al.*, 2010). In addition, AtISWI has been shown to have roles in gene silencing (Li *et al.*, 2012a), which may reflect a role for AtISWI in affecting the promoter regions. In the future it would be of interest to develop software for extracting information on how nucleosome distribution occurs in these regions, thus helping analyse the diverse functions of different types of remodelers.

EXPERIMENTAL PROCEDURES

Plant materials and growth conditions

Arabidopsis *chr11-1 chr17-1* mutant is in the Col-0 background and has been described previously (Li *et al.*, 2012a). Plant growth conditions were according to our previous methods (Xu *et al.*, 2003).

Nuclear extraction, MNase treatment and DNA purification

The nuclear extraction and MNase treatment were performed according to previously described methods (Zhang *et al.*, 2007; Shivaswamy *et al.*, 2008; Chodavarapu *et al.*, 2010; Weiner *et al.*, 2010; Sala *et al.*, 2011; Gaffney *et al.*, 2012; Li *et al.*, 2012b) with modifications. For nuclear extraction, 2-week-old Arabidopsis seedlings without roots were ground in liquid nitrogen and resuspended in lysis buffer [50 mM HEPES, pH7.5, 150 mM NaCl, 1 mM ethylenediaminetetraacetic acid (EDTA), 1% Triton X-100, 10% glycerol, 5 mM β-mercaptoethanol and protease inhibitor cocktail (Roche, https://www.roche-applied-science.com)]. After lysis for about half an hour, the lysis mixture was filtered through a 40-μm cell strainer (BD, https://www.bd.com/). The filtered plant extracts were centrifuged for 20 min at 3200 ***g*** to precipitate nuclei. Isolated nuclei were washed once with HBB buffer (25 mM Tris–HCl, pH 7.6, 0.44 M sucrose, 10 mM $MgCl_2$, 0.1% Triton-X and 10 mM β-mercaptoethanol) and once with HBC buffer (20 mM Tris–HCl, pH 7.5, 352 mM sucrose, 8 mM $MgCl_2$, 0.08% Triton-X, 8 mM β-mercaptoethanol and 20% glycerol). The obtained nuclei were resuspended with 100 μl of HBC buffer and flash frozen in liquid nitrogen.

For MNase treatment, the prepared nuclei were diluted into 900 μl of MNase digestion buffer [20 mM Tris–HCl, pH 8.0, 5 mM NaCl, and 2.5 mM $CaCl_2$] and divided into five portions. Each portion was digested with 4 U (final concentration of 0.02 U μl^{-1}) of MNase (TaKaRa, http://www.clontech.com/takara) for 15 min. The digestion was stopped by addition of 8 μl of 500 mM EDTA, and then treated with 80 μg of RNase A (Sigma, http://www.sigmaaldrich.com/) and 200 μg of Proteinase K (Roche), each for 1 h. DNA was purified with phenol/chloroform extraction and precipitated with salts and ethanol. Purified DNA was run on a 2% agarose gel, and bands corresponding to approximately 150 bp were cut and purified with a Gel Purification kit (Qiagen, http://www.qiagen.com/).

Deep sequencing

Approximately 1 μg of MNase-digested mononucleosome DNA was used for Illumina library generation following the manufacturer's instructions (Illumina, http://www.illumina.com/). Library construction and deep sequencing were performed by Genergy Biotechnology Co. Ltd. (Shanghai, China) using Illumina HiSeq 2000 following the manufacturer's instructions (Illumina). Raw data comprise 50 bp of single-end sequences.

Data analysis

For data analysis, FastQC (http://www.bioinformatics.babraham.ac.uk/projects/fastqc/) was used to examine the quality of sequencing reads. Based on the FastQC results, the first eight bases with irregular GC content and the last five bases with low sequencing quality were removed. The trimmed reads were mapped to the *A. thaliana* genome (TAIR10) using BOWTIE2.0 with default settings (Langmead *et al.*, 2009). To remove the potential bias caused by PCR amplification, only one copy of duplicated reads that mapped to exactly the same location was kept. Reads with low mapping quality (MAPQ < 20) were also discarded. As a result, 7 573 917 unique reads of Col-0 and 11 362 722 unique reads of *chr11-1 chr17-1* were obtained for further analysis, resulting in 13 and 19 reads per nucleosomes, respectively, on average (Table S1). Nucleosome positions were identified using the TEMPLATE FILTER software (http://compbio.cs.huji.ac.il/NucPosition/TemplateFiltering/Home.html) (Weiner *et al.*, 2010). Briefly, filtered reads were collapsed and prepared as required by the software, and seven pre-defined templates of both forward and reverse reads corresponding to nucleosomes as provided by the software website (Templates_7.1.txt) were used for detecting the position of nucleosomes. In this study, all major conclusions drawn based on nucleosome positions identified by TEMPLATE FILTER were repeatable using the raw reads (Figure S7), which have a relatively high background while maintaining the authentic biological signal, suggesting that TEMPLATE FILTER is also applicable to plant nucleosome position detection. For analysis of raw data, each read was extended to 150 bp (the expected length of nucleosome), and the center of the reads that are expected to be at the dyad position was used for further analysis. No extension was applied to the read for TEMPLATE FILTER analysis as the software infers the length of extension automatically (Figure S1).

The gene annotation file was downloaded from the TAIR homepage (http://www.arabidopsis.org). All genes could be divided into four major categories: 27 416 protein-coding genes, 31 189 TE, 3903 TE genes, and 924 pseudogenes. For nucleosome profile around the TSS, all gene regions are aligned such that the TSS across different genes are at the same position. The regions 1-kb up- and downstream of the TSS were divided into 40 bins. Bin size was set to 5 bp, and a 20 bin moving window was used for smoothing of the curve. The average nucleosome coverage for each group was first normalized by bin length and total nucleosome coverage (Read Per Kilobase Per Million Mapped Reads, RPKM) and was then calculated. Here, 'Read' represents the number of reads mapped to nucleosomes determined by TEMPLATE FILTER. For raw data analysis in Figure S7, the corresponding RPKM represents read number normalized by sequence length and sequencing depth.

Expression data has previously been published with Gene Expression Omnibus (GEO) accession GSE22159 (Li *et al.*, 2012a). RMA was used to normalize the datasets, and differentially expressed genes were defined based on combined criteria: $|FC| > 2$ and analysis of variance (ANOVA) $P < 0.01$.

To explore the relationship between nucleosome positioning and gene expression intensity, both Col-0 and *chr11-1 chr17-1* expression datasets were divided into four groups ranked by gene expression intensity, and the RPKM were calculated for each group. The DHS data have previously been published (Zhang *et al.*, 2012) and downloaded from GEO (GSE34318). Replication origin sequences were downloaded from a previous study (Costas *et al.*, 2011), and were aligned with TAIR10 using BLAST.

Accession Numbers

The MNase-seq data were deposited in the Gene Expression Omnibus (GEO, http://www.ncbi.nlm.nih.gov/geo/) under the accession number GSE50242.

ACKNOWLEDGEMENTS

We thank X. Cao for useful discussion of this study. This work was supported by grants from National Basic Research Program of China (973 Program, 2012CB910503) and the National Natural Science Foundation of China (90919040).

SUPPORTING INFORMATION

Additional Supporting Information may be found in the online version of this article.

Figure S1. Quality control of the MNase-seq data.

Figure S2. Data analysis pipeline.

Figure S3. Genes classified according to their expression levels.

Figure S4. Analysis of the AtISWI function in patterning nucleosomes.

Figure S5. Nucleosome distribution patterns in Col-0 and *chr11-1 chr17-1.*

Figure S6. Model for explaining the MNase-seq results in wild-type and *chr11-1 chr17-1.*

Figure S7. Major conclusions repeated using raw reads.

Table S1. Summary of the number of MNase-seq reads that are retained after the mapping and filtering processes.

REFERENCES

Aravind, L. and Iyer, L.M. (2012) The HARE-HTH and associated domains: novel modules in the coordination of epigenetic DNA and protein modifications. *Cell Cycle*, **11**, 119–131.

Bai, L. and Morozov, A.V. (2010) Gene regulation by nucleosome positioning. *Trends Genet.* **26**, 476–483.

Chen, K., Xi, Y., Pan, X., Li, Z., Kaestner, K., Tyler, J., Dent, S., He, X. and Li, W. (2013) DANPOS: dynamic analysis of nucleosome position and occupancy by sequencing. *Genome Res.* **23**, 341–351.

Chodavarapu, R.K., Feng, S., Bernatavichute, Y.V. *et al.* (2010) Relationship between nucleosome positioning and DNA methylation. *Nature*, **466**, 388–392.

Clapier, C.R. and Cairns, B.R. (2009) The biology of chromatin remodeling complexes. *Annu. Rev. Biochem.* **78**, 273–304.

Costas, C., de la Paz Sanchez, M., Stroud, H. *et al.* (2011) Genome-wide mapping of *Arabidopsis thaliana* origins of DNA replication and their associated epigenetic marks. *Nat. Struct. Mol. Biol.* **18**, 395–400.

Dong, J., Gao, Z., Liu, S., Li, G., Yang, Z., Huang, H. and Xu, L. (2013) SLIDE, the protein interacting domain of ISWI remodelers, binds DDT-domain proteins of different subfamilies in chromatin remodeling complexes. *J. Integr. Plant Biol.* **55**, 928–937.

Fincher, J.A., Vera, D.L., Hughes, D.D., McGinnis, K.M., Dennis, J.H. and Bass, H.W. (2013) Genome-wide prediction of nucleosome occupancy in maize reveals plant chromatin structural features at genes and other elements at multiple scales. *Plant Physiol.* **162**, 1127–1141.

Fu, K., Tang, Q., Feng, J., Liu, X.S. and Zhang, Y. (2012) DiNuP: a systematic approach to identify regions of differential nucleosome positioning. *Bioinformatics*, **28**, 1965–1971.

Gaffney, D.J., McVicker, G., Pai, A.A., Fondufe-Mittendorf, Y.N., Lewellen, N., Michelini, K., Widom, J., Gilad, Y. and Pritchard, J.K. (2012) Controls of nucleosome positioning in the human genome. *PLoS Genet.* **8**, e1003036.

Gkikopoulos, T., Schofield, P., Singh, V., Pinskaya, M., Mellor, J., Smolle, M., Workman, J.L., Barton, G.J. and Owen-Hughes, T. (2011) A role for Snf2-related nucleosome-spacing enzymes in genome-wide nucleosome organization. *Science*, **333**, 1758–1760.

Huanca-Mamani, W., Garcia-Aguilar, M., Leon-Martinez, G., Grossniklaus, U. and Vielle-Calzada, J.P. (2005) CHR11, a chromatin-remodeling factor essential for nuclear proliferation during female gametogenesis in *Arabidopsis thaliana*. *Proc. Natl Acad. Sci. USA*, **102**, 17231–17236.

Knizewski, L., Ginalski, K. and Jerzmanowski, A. (2008) Snf2 proteins in plants: gene silencing and beyond. *Trends Plant Sci.* **13**, 557–565.

Langmead, B., Trapnell, C., Pop, M. and Salzberg, S.L. (2009) Ultrafast and memory-efficient alignment of short DNA sequences to the human genome. *Genome Biol.* **10**, R25.

Langst, G. and Becker, P.B. (2001) Nucleosome mobilization and positioning by ISWI-containing chromatin-remodeling factors. *J. Cell Sci.* **114**, 2561–2568.

Li, G., Zhang, J., Li, J., Yang, Z., Huang, H. and Xu, L. (2012a) ISWI chromatin remodeling factors and their interacting RINGLET proteins act together in controlling the plant vegetative phase in Arabidopsis. *Plant J.* **72**, 261–270.

Li, Z., Gadue, P., Chen, K., Jiao, Y., Tuteja, G., Schug, J., Li, W. and Kaestner, K.H. (2012b) Foxa2 and H2A.Z mediate nucleosome depletion during embryonic stem cell differentiation. *Cell*, **151**, 1608–1616.

Narlikar, G.J. (2010) A proposal for kinetic proof reading by ISWI family chromatin remodeling motors. *Curr. Opin. Chem. Biol.* **14**, 660–665.

Russo, V.E.A., Martienssen, R.A. and Riggs, A.D. (1996) *Epigenetic Mechanisms of Gene Regulation*. Woodbury: Cold Spring Harbor Laboratory Press.

Sadeh, R. and Allis, C.D. (2011) Genome-wide "re"-modeling of nucleosome positions. *Cell*, **147**, 263–266.

Sala, A., Toto, M., Pinello, L., Gabriele, A., Di Benedetto, V., Ingrassia, A.M., Lo Bosco, G., Di Gesu, V., Giancarlo, R. and Corona, D.F. (2011) Genome-wide characterization of chromatin binding and nucleosome spacing activity of the nucleosome remodelling ATPase ISWI. *EMBO J.* **30**, 1766–1777.

Shivaswamy, S., Bhinge, A., Zhao, Y., Jones, S., Hirst, M. and Iyer, V.R. (2008) Dynamic remodeling of individual nucleosomes across a eukaryotic genome in response to transcriptional perturbation. *PLoS Biol.* **6**, e65.

Smaczniak, C., Immink, R.G., Muino, J.M. *et al.* (2012) Characterization of MADS-domain transcription factor complexes in *Arabidopsis* flower development. *Proc. Natl Acad. Sci. USA*, **109**, 1560–1565.

Stroud, H., Otero, S., Desvoyes, B., Ramirez-Parra, E., Jacobsen, S.E. and Gutierrez, C. (2012) Genome-wide analysis of histone H3.1 and H3.3 variants in *Arabidopsis thaliana*. *Proc. Natl Acad. Sci. USA*, **109**, 5370–5375.

Struhl, K. and Segal, E. (2013) Determinants of nucleosome positioning. *Nat. Struct. Mol. Biol.* **20**, 267–273.

van Dijk, K., Ding, Y., Malkaram, S. *et al.* (2010) Dynamic changes in genome-wide histone H3 lysine 4 methylation patterns in response to dehydration stress in *Arabidopsis thaliana*. *BMC Plant Biol.* **10**, 238.

Weiner, A., Hughes, A., Yassour, M., Rando, O.J. and Friedman, N. (2010) High-resolution nucleosome mapping reveals transcription-dependent promoter packaging. *Genome Res.* **20**, 90–100.

Xu, L., Xu, Y., Dong, A., Sun, Y., Pi, L. and Huang, H. (2003) Novel *as1* and *as2* defects in leaf adaxial-abaxial polarity reveal the requirement for *ASYMMETRIC LEAVES1* and *2* and *ERECTA* functions in specifying leaf adaxial identity. *Development*, **130**, 4097–4107.

Yadon, A.N. and Tsukiyama, T. (2011) SnapShot: chromatin remodeling: ISWI. *Cell*, **144**, 454–454.e451.

Yadon, A.N., Van de Mark, D., Basom, R., Delrow, J., Whitehouse, I. and Tsukiyama, T. (2010) Chromatin remodeling around nucleosome-free regions leads to repression of noncoding RNA transcription. *Mol. Cell. Biol.* **30**, 5110–5122.

Zhang, X., Clarenz, O., Cokus, S., Bernatavichute, Y.V., Pellegrini, M., Goodrich, J. and Jacobsen, S.E. (2007) Whole-genome analysis of histone H3 lysine 27 trimethylation in *Arabidopsis*. *PLoS Biol.* **5**, e129.

Zhang, W., Zhang, T., Wu, Y. and Jiang, J. (2012) Genome-wide identification of regulatory DNA elements and protein-binding footprints using signatures of open chromatin in *Arabidopsis*. *Plant Cell*, **24**, 2719–2731.